ISSN 2395-1621

Investigation and flow visualization of Electrostatic Precipitator (ESP)

[#1] Mr. Alok S. Chaudhary, [#2]Prof. (Mrs.) Anita A. Nene

[1]alokchaudhary24@gmail.com
[2] anita.nene@mitpune.edu.in

[#1]Department of Mechanical Engineering, Maharashtra Institute of Technology, Pune, India

ABSTRACT

The particulate matters from most of the industries such as boiler, cement, power generation etc. received attention because of firm environmental protection agency (EPA) regulations. Electrostatic precipitators (ESP) developed by Frederick G. Cottrell (Professor of chemistry at the University of California, Berkeley) is the most common, operative and consistent technologies for removal of hazardous emissions. Objective of this work is to properly distribute the flow pattern and study of different boundary conditions on flow pattern to calculate the pressure drop across the electrostatic precipitator. In this present paper, to visualize the flow in ESP Computational Fluid Dynamics (CFD) is used for simulation. A four module ESP is selected for the case study. The flow visualization in ESP is assessed under the modified geometric conditions such as Gas Distribution (GD) Screen, Hopper Baffle, Gas Distribution (GD) vanes, Duct Vanes. Also effect of different boundary conditions such as varying flow rate, temperature, and fine mesh is studied. The simulation results shows that by using appropriate opening of GD screen, hopper baffle and GD vanes uniform distribution of flow across ESP is obtained.

Keywords— Electrostatic Precipitator(ESP), Gas Distribution (GD) Screen, Computational Fluid Dynamics (CFD).

ARTICLE INFO

Article History

Received : 23th May, 2015

Received in revised form :

25th May, 2015

Accepted : 28th May, 2015

Published online :

1st June 2015

I. INTRODUCTION

The particle emissions from industries such as cement, boilers have been drawing more attention due strict environmental protection agency (EPA) regulations [1]. Industrial pollutants can be reduced by its conservation or retrieval. The Electrostatic Precipitator's (ESP's) are extensively used for cleaning flue gases from process industries. They can work in comprehensive range of gas temperature with efficiency 99.9 % as compared to other mechanical devices such as cyclones and bag filters. The ESP involved some complex and interconnected physical mechanism like particle charging, particle collection and removal of collection dust by rapping mechanism. Due to corona discharge ionic and electronic charging of gas particles which are moving in Electro hydrodynamic field took place and charged particles are moved toward collecting plates [2].

Flow distribution inside the ESP has variable effect on its collection efficiency, which depends upon the geometric structures inside ESP such as GD screen opening, baffle plates, GD vanes. It is tough enough to analyse detail and consistent measurement of fluid flow behaviour and pressure drop for an ESP as the geometric structure is very intricate. CFD plays a vital role for ensuring uniform gas & dust flow distribution within ESP fields. Avoids extensive, repetitive Trial -&-Error (T&E) method on field erected ESP, for ensuring uniform gas velocity inside ESP. Precise CFD model plays an important role in visualization of fluid flow inside ESP along with pressure drop calculations. However, there is limited research has been done on analysis of turbulent flow in the ESP. Shah et al. [3] studied the lab scaled ESP to optimize its flow distribution by using CFD. Haywood et al. [4] optimizes the flow pattern for the two ESPs within given limitations. Dumont and Mudry [5] analysed the simulation outcomes of ten different ESP models to make a comparative study on fluid flow inside

ESP. Researchers also studied the two dimensional basic ESP models and overlooked the effect of sudden expansion in structural outline of an ESP.

The aim of the work is to obtain the uniform flow by simulation analysis results. Flow visualizations inside ESP are modelled numerically using CFD. The modelling and meshing was done by using ICEM and for solver purpose ANSYS FLUENT is used. It is to be noted that all the GD screens, hopper baffles, GD vanes, duct vanes etc. are taken into account in this CFD model except the collecting electrode as it will not affect the fluid flow. For the optimization of uniform flow and pressure drop calculation comprehensive numerical approach and simulation method is presented. The simulation results are analysed and possible modification are done to meet standards set by Institute of Clean Air Companies (ICAC).

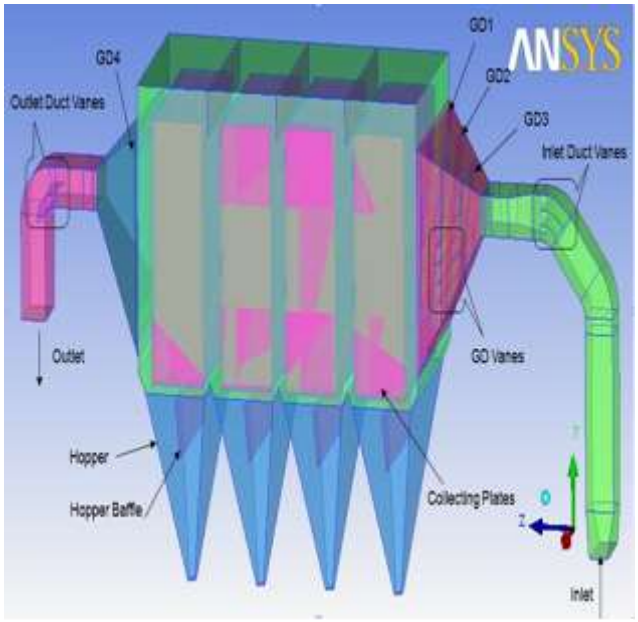

Fig. 1: Typical 4 Module ESP Geometry.

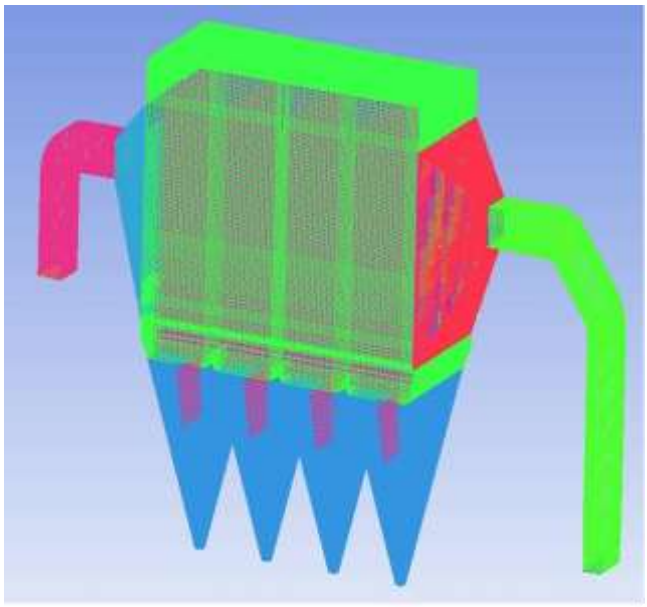

Fig. 2: Computational Mesh of an ESP.

II. ESP SYSTEM DESCRIPTION

The dimensions of the four module ESP is obtained from the supplier in Auto Cad sheet. The main components of the ESP are considered while modelling the ESP using Ansys ICEM 13.5. The main components are inlet, outlet, GD screen, GD vanes, hopper baffle, straightening vanes etc. illustrated in Fig. 1. The ducting is connected at both inlet and outlet. The ESP model is drawn in 3D shows full scale geometry and operation temperature, so no scaling or correction factor for density was required. Blocking is used for meshing purpose to create the Hexa mesh illustrated in Fig. 2. This contains 3472497 computational cells.

III. GD SCREEN MODELLING

Different parameters such as porous jump coefficient C_2 and face permeability α of GD screen are generally Calculated from experimental and mathematical modelling. Sometimes simulation of unit cell is carried out. For the GD screen, the simulation of unit cell can be a representative fluid flow domain around the single hole, due to the repeated Pattern of GD screen [6]. Fig.3 shows the typical layout of GD screen. Part of these GD is considered as a unit cell for the calculation of porous jump coefficient as shown in Fig 4. There are different opening for GD screen such as 23 %, 30%, 40% and 50%. The diameters of the holes in the GD screen are constant only pitch is variable for different openings. As the percentage opening increases the pitch hole are decreasing.

The model is pre-processed in ICEM, simulated and post processed in Ansys Fluent. Symmetry boundary conditions are used during simulation because unit cell has repeated pattern. For all the simulations in this paper turbulent flow is considered and two-equation k-ε model is used. In CFD simulation GD screen are simulated as a thin membrane for which velocity pressure drop characteristics are known. Porous media of finite thickness with permeability over which the pressure drop is defined is a combination of Darcy's Law and an additional inertial loss term is given by [1]

$$\Delta P=\{\frac{\mu}{\alpha}\, v + c_2\, \frac{1}{2}\, \rho v^2\}\Delta m \quad (1)$$

For the above equation, detailed information is accessed from Fluent user guide (ANSYS 13).

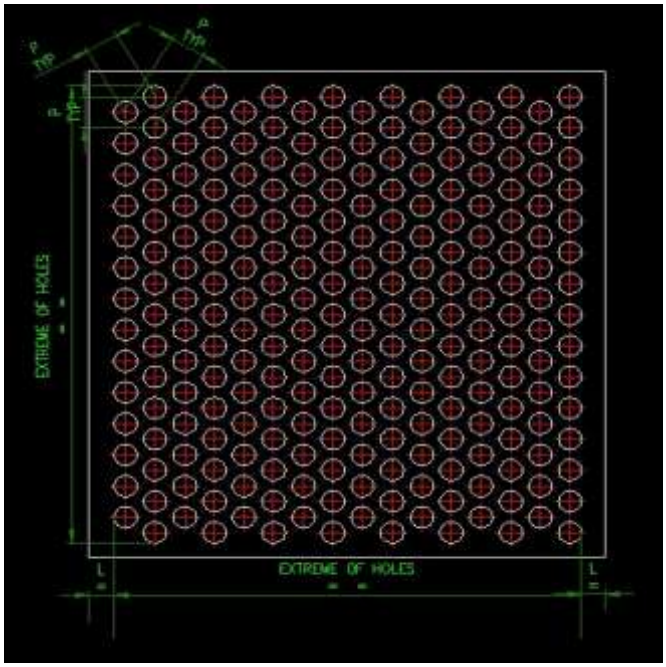

Fig. 3: Gas Distribution (GD) Screen layout.

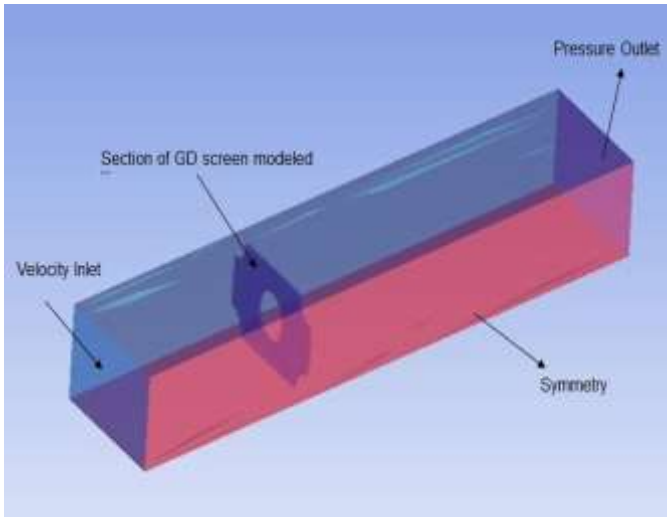

Fig. 4: Selection of unit cell from GD screen.

For each percentage opening separate unit cell of GD screen is modelled and simulation is carried for different velocity to calculate the pressure drop across inlet and outlet which is occurred due to inertial loss at turbulent flow. Fig 4 shows a modelled and mesh file of unit cell of a 30 % opened GD screen. Hexa mesh is created for the simulation. The simulation is carried out for all openings as stated above and from the results graph is plotted. The corresponding parameters such as porous jump coefficient C_2 and face permeability α are obtained by curve fitting given in Table 1. A second degree polynomial curve is obtained for every opening and it is solved for equation (1). Fig 5 shows that pressure drop increased with increase in inlet velocity and reduction in porosity.

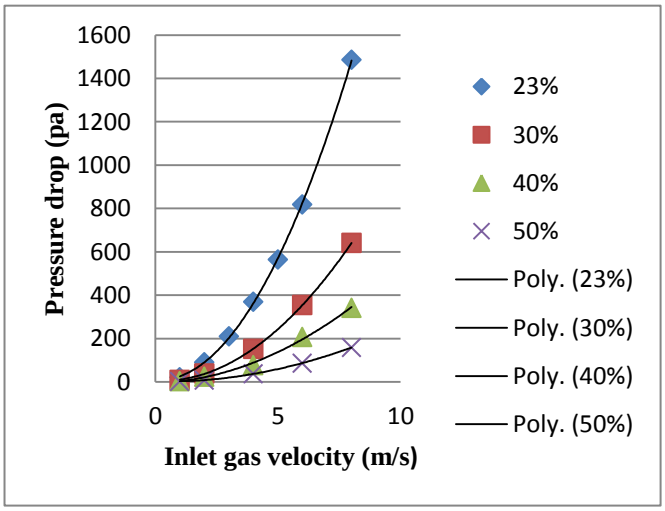

Fig. 5: Relations between inlet gas velocity and pressure drop for different GD percentage opening.

Sr. No.	GD % opening	Face Permeability α (m^2)	porous jump coefficient C_2 (m^{-1})
1	23	2.10E-08	12763
2	30	2.13668E-08	5614
3	40	7.36177E-08	2896
4	50	9.35389E-08	1360

Table 1: Porous jump Coefficient and Face Permeability values for different percentages of GD openings.

IV. NUMERICAL APPROACH AND SIMULATION PROCEDURE

In the numerical computation of ESP, the fluid flow includes conservation of mass, momentum and turbulence model equations.

A. Governing Equations

Air is used as a working fluid inside the ESP. It is considered as incompressible Newtonian fluid flow which is governed by conservation of mass equation [1] given by

$$\frac{\partial \rho}{\partial t} + \vec{\nabla}.\left(\rho \vec{U}\right) = 0 \quad (2)$$

and the momentum equation is given by,

$$\frac{\partial \vec{U}}{\partial x} + \vec{U}\vec{\nabla}\vec{U} = -\frac{\vec{\nabla}p}{\rho} + v\vec{\nabla}^2\vec{U} + \vec{g}\frac{\partial \rho}{\partial t} + \vec{\nabla}\left(\rho \vec{U}\right) = 0 \quad (3)$$

Exact picture of turbulent flow activities inside the ESP is crucial for success of CFD. There are different turbulent models that can be used for simulation in fluent such as Reynolds stress model, k-ω model, k- ε model etc. in this study k- ε is used, as the model is simple to setup and widely used in most of the industries. k- ε model comprises of turbulent viscosity and transport equation for dissipation rate[7]. Governing equation of k- ε model is shown below:

$$\frac{\partial}{\partial t}(\rho k) + \frac{\partial}{\partial x_j}(\rho k u_j) \quad (4)$$
$$= \frac{\partial}{\partial x_j}\left[\left(\mu + \frac{\mu_t}{\sigma_k}\right)\frac{\partial k}{\partial x_j}\right] + G_k + G_b + \rho\varepsilon - Y_m + S_k$$

$$\frac{\partial}{\partial t}(\rho\varepsilon) + \frac{\partial}{\partial x_j}(\rho\varepsilon u_j) = \quad (5)$$
$$\frac{\partial}{\partial x_j}\left[\left(\mu + \frac{\mu_t}{\sigma_k}\right)\frac{\partial \varepsilon}{\partial x_j}\right] + \rho c_1 s_{\delta -} \rho c_0 \frac{\varepsilon^2}{k+\sqrt{v\varepsilon}} +$$
$$c_{1\delta}\frac{\varepsilon}{k}c_{3\delta}G_b + S_\delta$$

Where,

$$c_1 = max\left[0.43\frac{\eta}{\eta+5}\right], \eta = s\frac{k}{\varepsilon}, s = \sqrt{2s_{ij}s_{ij}}$$

The ratio of RMS velocity fluctuations to mean flow velocity is called as turbulence intensity and that can be calculated from the following formula which is derived from empirical correlation for pipe flow [8],

$$I = \frac{u'}{u_{avg}} = 0.16(Re_{Dh})^{-1/8} \quad (6)$$

B. Boundary Conditions

3D geometry model as shown in Fig 1was considered for the simulation purposed. Air is used as a working Fluid. For the discretization of the PDE's finite volume method was used. SIMPLE solution method scheme was applied for pressure-velocity couplings and first order upwind scheme was employed to interpolate variables on surface of control volume. Number of simulations was performed with different geometric modification to obtained uniform flow and low pressure drop. The velocity inlet boundary condition is employed to Inlet of ESP. velocity is calculated from the flow rate and comes out to be 20.07m/s. For the outlet of ESP, pressure outlet boundary condition is applied with zero gauge pressure. No slip boundary conditions are selected in all walls in ESP. turbulent kinetic energy and dissipation rate are selected as unity in inlet boundary conditions. Working temperature is selected as 180^0c and as per working temp dynamic viscosity and density is selected. Porous jump values are defined for the GD screens.

C. GD Screen Opening Percentage

The simulation of ESP was performed for the optimisation of GD screen. As per the nozzle inlet opening (IOR) ratio the different opening percentage was defined for the different GD screen such as GD1, GD2, GD3 and GD4. IOR ratio of the precipitator is calculated from width of the inlet opening of ESP to that of height of inlet opening. GD 3 is set to all 40 % opening. Top 3/8 portion of GD2 is set to 50 % opening, middle 3/8 portion is 40 % opened and remaining portion of GD 2 is set to 30 %. GD 1 opening is as shown in Fig 5. It is not possible to draw GD screen as per Fig 3 because mesh count will be high and it will take much time for calculation so simple plain is drawn and porosity is set as per opening.

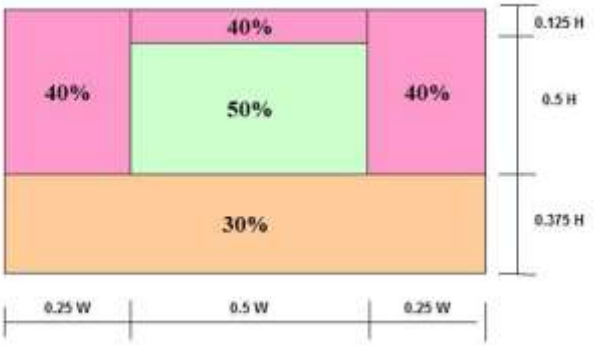

Fig. 5: Opening Percentage for GD Screen 1.

V. DATA ASSESSMENT AND FIELD TESTING METHODS

Results obtained from the simulation can be compared with the field testing data. There are different statistical techniques to compare the CFD results. We can improve the flow pattern with the help of velocity and vector contours.

For the data comparison with actual field results generally a rake is created at the end of first field as shown in Fig 6. The velocity distribution at the end of the first field is plotted in Microsoft excel and generally quantified in following ways

a. Particular standards are set by Institute of Clean Air Companies (ICAC). According to the at the end of first field in collection compartment the velocity readings shall have a 85 % of velocities are not more than 1.15 times avg. velocity and 99 % are not more than 1.40 times avg. velocity[5].

(a)

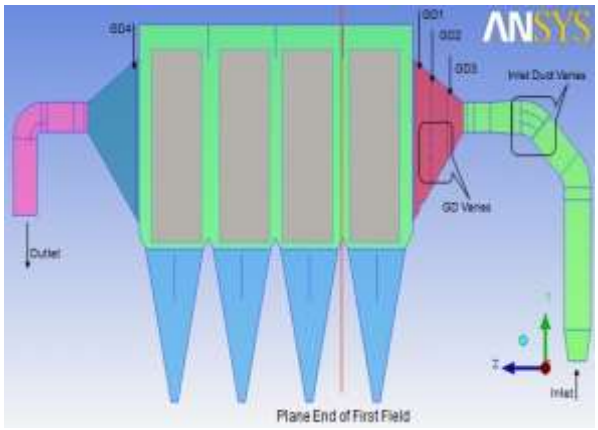

(b)

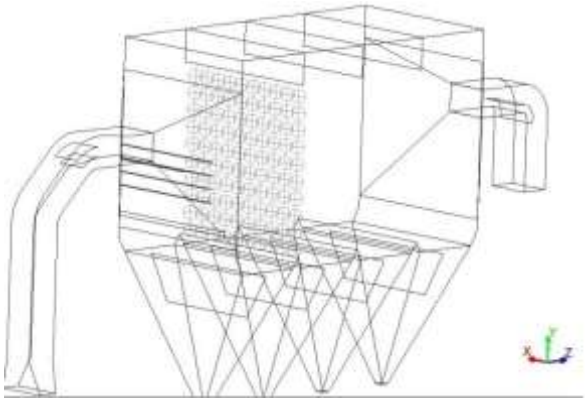

Fig. 6 (a) Measurement plane for velocity calculation (b) Rake created for velocity measurement

b. The precent RMS is calculated by the following formula

$$\% \text{ RMS} = \frac{100}{V_{avg}} \sqrt{\frac{\sum (V_i - V_{avg})^2}{(\sum i) - 1}}$$

Where,

V_i = Velocity at selected grid point in rake

V_{avg} = average velocity over entire rake

i= grid point counter

The typical goal in industry is to reach a % RMS of less than 15% at the ESP inlet and outlet planes. We measured RMS value at the end of first field.

VI. RESULT AND DISCUSSION

The geometry of ESP as shown in Fig. 2 consists of 3472497 computational cells. The grid independency test was checked and simulation is completed with Core i7 3.1 GHz 64 bit CPU with 8 GB RAM and 160 GB hard disc memory.

a. GD Optimization

Simulation and post processing of ESP is done in Fluent for the GD optimization. Sixteen simulations are carried out for the modification of GD opening percentage. Fig. 7 shows the velocity contour of ESP at the end of first field before modification. We can conclude that flow pattern is not uniform; velocity is more in the corners of ESP chamber. Fig. 8 shows the velocity vector contour for GD pattern as discussed earlier. The vortex formation is more and the maximum flow is flowing through hopper. The flow has highest velocity at top of collection chamber.

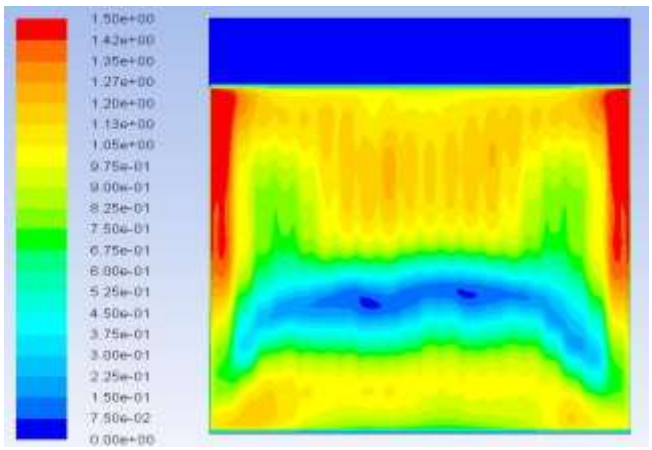

Fig. 7: Velocity contour at end of first field
(Before GD screen Modification)

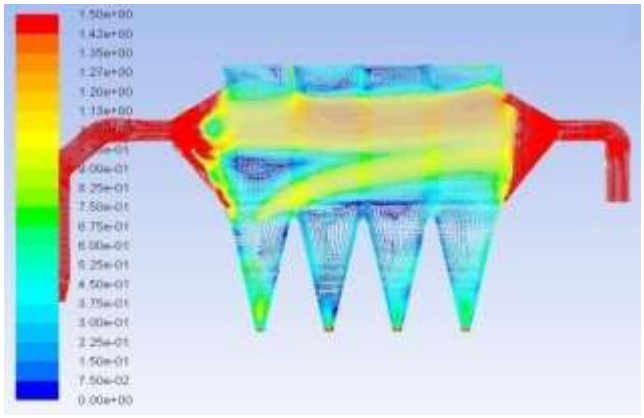

Fig. 8: Velocity contour at vertical mid-section of ESP
(Before GD screen Modification)

After the modification of GD screen final percentage of GD screen opening is as shown in Fig 9. Opening percentage for GD 1 is kept 40 %and outlet GD is kept as it is. Fig 10 shows the velocity contour at end of first field after GD modification which shows uniform distribution of flow. Fig 11 shows the velocity vector contour after GD modification, the flow is in straight direction with less number of vortex formation.

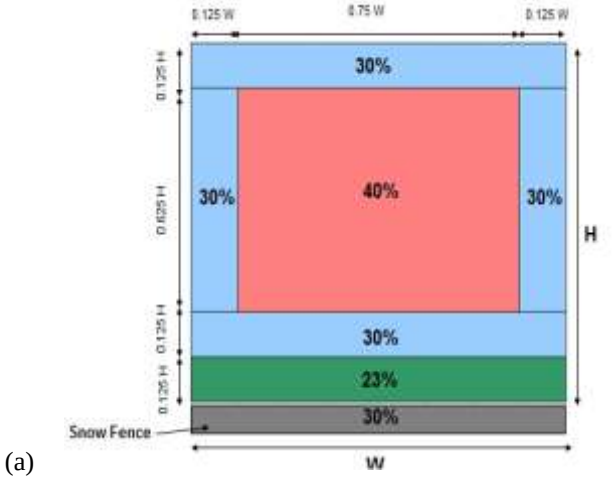

(a)

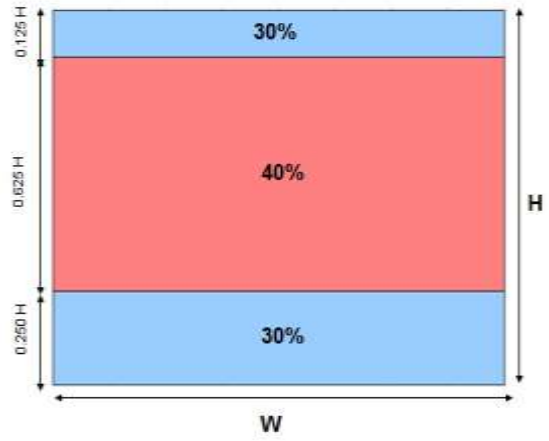

(b)

Fig. 9 Modified GD opening Percentage (a) GD Screen 1 (b) GD Screen 2

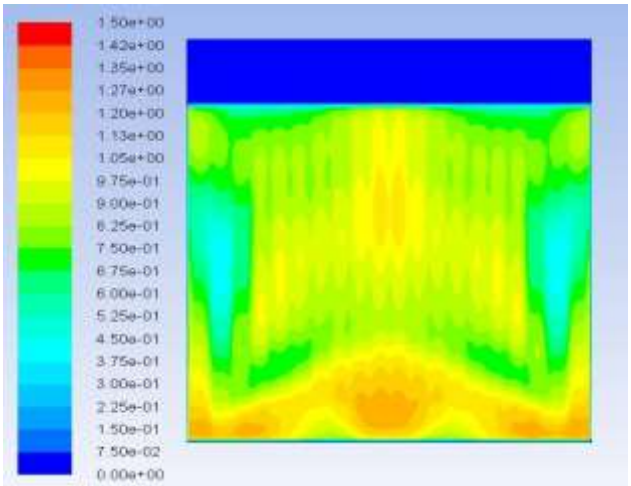

Fig. 10: Velocity contour at end of first field
(After GD screen Modification)

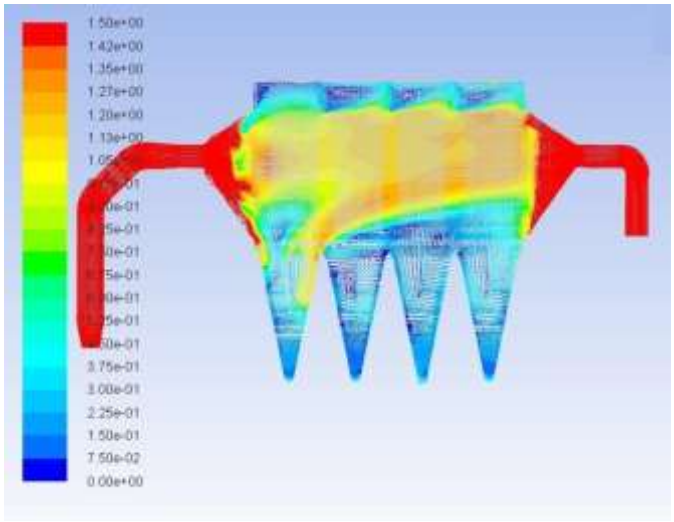

Fig. 11: Velocity contour at vertical mid-section of ESP (After GD Screen Modification)

As per ICAC guidelines 81 % of velocity readings are within 1.15 time's average velocity and 95 % of velocity readings are within 1.40 average velocity. Total pressure drop for previous case was Total pressure drop across ESP was 20.2 mm WC at 180^0c.

b. Stimulation with Geometric Modifications

Two simulations are carried for the ESP. one is done with all the geometric modifications and other is without geometric modifications. Geometric modification includes the Hopper Baffle, Duct vanes and GD vanes. GD Screen opening is kept as per site. Fig 12 shows the comparison of velocity contour at the end of first field and bottom figure shows the contour after geometric modifications are made inside ESP. Based on Fig. 12 (a), the high velocity occurs at center and corners of collection chamber at end of first field.

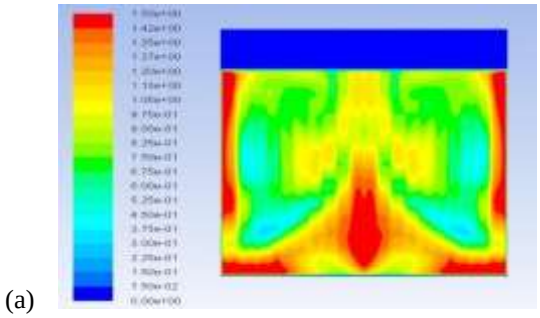

(a)

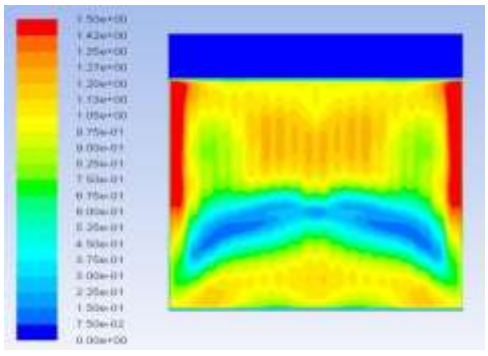

(b)

Fig. 12 Plane End of First Field (a) without geometric modification in ESP (b) with geometric modification in ESP

Fig. 13 shows the velocity vector for both the simulations. Based on Fig. 13 (a), maximum flow is entering into the first hopper due to which vortex formation increases and fluid flow is passing through the upper portion in the collection chamber. Dur to geometric modification added into the ESP fluid is flowing straight in collection chamber.

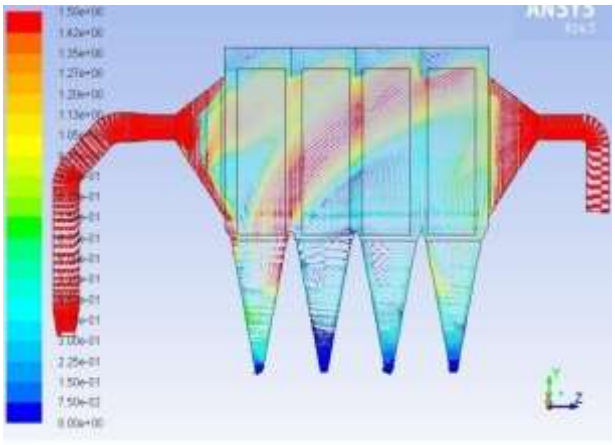

(a)

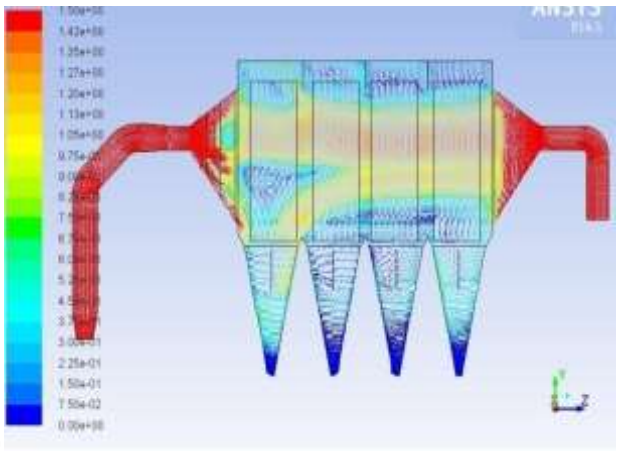

(b)

Fig. 13: Velocity contour at vertical mid-section of ESP (a) without geometric modification in ESP (b) with geometric modification in ESP

Fluid flow is showing low velocity region in bottom side of ESP. the average velocity at the end of first field is 0.89 m/s. Due to geometric modification total pressure reduces by 23 mm WC.

VII. CONCLUSION

The whole work is mainly divided into three stages i.e. modelling and simulation of unit cell of GD screen to calculate porosity values, optimization of GD screen and analysis of whole ESP with geometric modification in it. Porous jump values are calculated for the different opening of GD screen. These values can be used for any ESP simulation. k-ε model was used for calculating computing turbulence. Velocity readings inside ESP are compared with site readings and they are found in reasonable agreement. The model with geometric modifications shows uniform flow pattern as per guidelines of ICAC.

NOMENCLATURE

C_2 Pressure jump coefficient = Pressure loss coefficient per unit thickness (m-1)

g	Gravity (m/ s^2)
G_k	Generation of turbulence kinetic energy due to the mean velocity gradients (m2/s2)
G_b	Generation of turbulence kinetic energy due to buoyancy (m2/s2)
I	Intensity
k	Turbulent kinetic energy (m2/s2)
Δm	Thickness of the perforated plate (m)
p	Pressure (Pa)
U	Velocity (m/s)
S_k , Sε	User-defined source terms
S	Modulus of the mean rate of strain tensor
u′	Fluctuating velocity (m/s)
u_{avg}	Average velocity (m/s)
Y_M	Contribution of the fluctuating dilatation in compressible turbulence to the overall dissipation rate

Greek symbols

α	Permeability of the perforated plate (m2)
Δ	Differential
ε	Turbulent dissipation rate (m2/s3)
η	Strain
μ	Dynamic viscosity (N.s/ m2)
ν	Kinematic viscosity (m2/s)
ρ	Density (kg/m3)
σ_k	Turbulent Prandtl numbers for *k*
σε	Turbulent Prandtl numbers for ε

REFRENCES

[1] Shah M. E. Haque, M. G. Rasul, M. M. K. Khan, A. V. Deev, and N. Subaschandar, "Numerical modelling for optimizing flow distribution inside an electrostatic precipitator", International journal of mathematics and computers in simulation, Issue 3, Volume 1, 2007.

[2] S.H. Kim, K.W. Lee, "Experimental study of electrostatic precipitator performance and comparison with existing theoretical prediction models", Journal of Electrostatics 48 (1999) 3-25.

[3] Shah M. E. Haque, M. G. Rasul, M. M. K. Khan, A. V. Deev, and N. Subaschandar, "Numerical modelling for optimizing flow distribution inside an electrostatic precipitator", International journal of mathematics and computers in simulation, Issue 3, Volume 1, 2007.

[4] R.J Haywood, G.J. Brown, L.J. Irons, M. Stark, " Using CFD to reduce commissioning time for Electrostatic Precipitators", Fifth International Conference on CFD in the Process Industries CSIRO, Melbourne, Australia, December 2006.

[5] B. J. Dumont and R. G. Mudry, "Computational fluid dynamic modeling of electrostatic precipitators", Proceedings of electric power conference, 2003.

[6] Q. F. Hou, B.Y. Guo, L.F. Li and A. B. Yu, "Numerical simulation of gas flow in an Electrostatic Erecipitator", Seventh International Conference on CFD in the Minerals and Process Industries CSIRO, Melbourne, Australia 9-11 December 2009.

[7] A. F. Yusop, R. Mamat, M. H. Mat Yasin, and S. Suhaimi, "Effects of the Inlet Velocity Profiles on the Prediction of Velocity Distribution inside an Electrostatic Precipitator (ESP)", International Journal of Computer and Electrical Engineering, Vol. 6, No. 1, February 2014.

[8] Fluent 6.2 User's Guide, Fluent Inc., 2005.